

## Synthesis, Biodistribution, and Microsingle Photon Emission Computed Tomography (SPECT) Imaging Study of Technetium-99m Labeled PEGylated Dendrimer Poly(amidoamine) (PAMAM)–Folic Acid Conjugates

Yuanqing Zhang,<sup>†,‡</sup> Yanhong Sun,<sup>†</sup> Xiaoping Xu,<sup>†,‡</sup> Xuezhu Zhang,<sup>†,‡</sup> Hua Zhu,<sup>†,‡</sup> Liliang Huang,<sup>†,‡</sup> Yujin Qi,<sup>†</sup> and Yu-Mei Shen<sup>\*,†,§</sup>

<sup>†</sup>Shanghai Institute of Applied Physics, Chinese Academy of Sciences, 2019 Baojia Road, Shanghai 201800, China, <sup>‡</sup>Graduate School of the Chinese Academy of Sciences, 19 Yuquan Road, Beijing 100049, China, and <sup>§</sup>Shanghai Center for Systems Biomedicine, Shanghai Jiao Tong University, 800 Dongchuan Road, Shanghai 200240, China

Received December 23, 2009

Three conjugates based on dendrimer PAMAM generation five were synthesized and radiolabeled successfully. To investigate their tumor targeting, the *in vitro* and *in vivo* stability, cell uptake, *in vivo* biodistribution, and micro-SPECT imaging were evaluated, respectively. The conjugate of <sup>99m</sup>Tc labeled PEGylated dendrimer PAMAM folic acid conjugate (<sup>99m</sup>Tc-G5-Ac-pegFA-DTPA) shows much higher uptake in KB cancer cells and accumulated more in the tumor area than that of the other two conjugates. The uptake in KB cells depends on the incubation time. The results of *in vivo* biodistribution agree with the data obtained from micro-SPECT imaging. These studies show that PEGylation of PAMAM dendrimer folic acid conjugate improves the tumor targeting. Folate-conjugated dendrimer maybe developed to be potential radiopharmaceuticals and targeted drug delivery systems.

### Introduction

Nanoparticles are able to accumulate within tumor tissue due to the widely reported enhanced permeation and retention (EPR<sup>4</sup>) effect which relies on the passive accumulation of colloidal macromolecules of 40 kDa and above in tumors.<sup>1,2</sup> The EPR effect arises due to aberrant tumor endothelium, which is a result of its “leakiness”, allows the penetration into tumor tissue. Dendrimers are artificial macromolecules with tree-like structures.<sup>3–6</sup> They are hyperbranched and monodisperse three-dimensional molecules with defined molecular weights and host–guest entrapment properties. Dendrimers are synthesized from branched monomer units in a stepwise manner, thus it is possible to precisely control their molecule properties, such as size, shape, dimension, density, polarity, flexibility, and solubility, by choosing different building/branching units and surface functional groups.<sup>7</sup> Furthermore, the large numbers of surface functional groups on dendrimer’s outer shell can be modified or conjugated with a variety of interesting guest molecules. These specific properties make dendrimers suitable for drug delivery systems. In the recent years, increasing interest has been attracted to the application

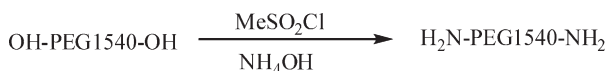
of dendrimers as targeting carriers in cancer therapy and imaging. It is well established that the conjugation of special targeting moieties to dendrimers can lead to preferential distribution of the cargo in the targeted tissue or cells. Examples of these special targeting moieties include folic acid,<sup>8–10</sup> antibody,<sup>11,12</sup> peptide,<sup>13</sup> and epidermal growth factor.<sup>14,15</sup>

Folate receptors (FR), which are 38 kDa glycosylphosphatidylinositolanchored proteins, exist in three major forms, namely FR- $\alpha$ , FR- $\beta$ , and FR- $\gamma$ . The FR- $\alpha$  form is overexpressed in many types of tumors including ovarian, endometrial, breast, renal cell carcinomas, and so forth. The fact that high affinity FR binding is retained when folate is covalently linked via its  $\gamma$ -carboxyl group to a foreign molecule, combined with the prevalence of FR overexpression among tumors, so folate-based targeting systems present an effective means of selectively delivering therapeutic or imaging agents to tumors.<sup>16–20</sup> Folate-targeted technology has been successfully applied to drug delivery, therapeutic agents, MRI contrast agents, and gadolinium liposomes and radioimaging of cancer cells.<sup>21–30</sup>

A lot of literature has already reported that dendrimer folic acid conjugates were fluorescein labeled and bioevaluated.<sup>8–10</sup> However, the fluorescein labeled dendrimer conjugates is very difficult to be detected in a live animal study. At the same time, radiolabeled dendrimer conjugates is very convenient in small animal single photon emission computed tomography (SPECT) or positron emission tomography (PET) imaging studies. The conjugate of dendrimer monoclonal antibodies conjugates have been radiolabeled with <sup>111</sup>In or <sup>153</sup>Gd or <sup>125</sup>I radionuclides.<sup>31–34</sup> Radiolabeled dendrimer–biotin and dendrimer–avidin conjugates were also investigated *in vivo*.<sup>35,36</sup> To the best of our knowledge, the live animal micro-SPECT

\*To whom correspondence should be addressed. Phone: +86-21-39194692. Fax: +86-21-39194691. E-mail: shenyumei@sinap.ac.cn.

<sup>a</sup> Abbreviations: PAMAM, poly(amidoamine); EPR, enhanced permeability and retention; FA, folic acid; FR, folate receptors; SPECT, single photon emission computed tomography; PET, positron emission tomography; PEG, poly(ethylene glycol); NHS, *N*-hydroxysuccinimide; DCC, *N,N*-dicyclohexyl carbodiimide; EDC, 1-[3-(dimethylamino)propyl]-3-ethylcarbodiimide HCl triethylamine; DMSO, dimethyl sulfide; DMF, dimethylformamide; 1B4M-DTPA, 2-(*p*-isothiocyanatobenzyl)-6-methyl-diethylenetriaminepentaacetic acid; ACN, acetonitrile; TFA, trifluoroacetic acid.

**Scheme 1.** Synthesis of Diaminopolyoxyethylene1540<sup>a</sup>

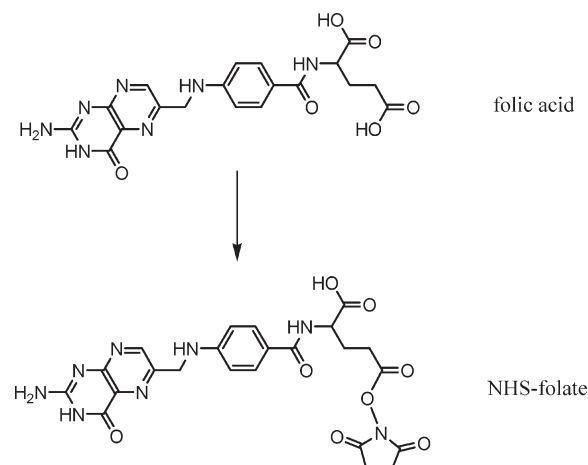
<sup>a</sup> Reagents and conditions: (1) CH<sub>3</sub>SO<sub>2</sub>Cl, Et<sub>3</sub>N, CH<sub>2</sub>Cl<sub>2</sub>, rt, 12 h; (2) NH<sub>4</sub>OH, rt, 48 h.

imaging study of the dendrimer complex has not been reported so far. Technetium-99m is so far the most commonly used radionuclide in nuclear imaging. More than 80% of all usually used radiopharmaceuticals contain this short-lived metastable radionuclide. This is due to the highly interesting physical properties of <sup>99m</sup>Tc among which are its short half-life (6 h) and  $\gamma$  photon emission of 140 keV, which is very important for both effective imaging and patient safety perspectives. Technetium-99m can be derived as a column elute from a <sup>99</sup>Mo/<sup>99m</sup>Tc generator, which makes it readily available.<sup>37</sup> Furthermore, <sup>99m</sup>Tc possesses latent chemical properties, facilitating thereby the labeling of several types of kits for versatile diagnostic applications. Recently, we reported radiolabeled dendrimer folic acid conjugate has certain accumulation in KB tumor tissue.<sup>38</sup> To bind efficiently with the folate receptor positive tumors, the structure of the dendrimer folic acid conjugate was modified by PEGylation. Both of the biodistribution and micro-SPECT imaging study revealed that the PEGylated conjugate has highest concentration on the tumor while the radiolabeled dendrimer without folic acid shows the lowest accumulation in the three conjugates, which will be described in this paper. Herein we report our detailed results on radiolabeled dendrimer conjugates for potential SPECT imaging agent.

**Results**

**Chemistry.** PEG bis amine (NH<sub>2</sub>-PEG 1540-NH<sub>2</sub>) was synthesized in two successive steps (Scheme 1) in which PEG-1540 was converted to CH<sub>3</sub>SO<sub>2</sub>-PEG 1540-SO<sub>2</sub>CH<sub>3</sub> using CH<sub>3</sub>SO<sub>2</sub>Cl, then CH<sub>3</sub>SO<sub>2</sub>-PEG 1540-SO<sub>2</sub>CH<sub>3</sub> was converted to NH<sub>2</sub>-PEG 1540-NH<sub>2</sub> using ammonia hydroxide. PEG bis amine synthesis was confirmed by IR spectroscopy and <sup>1</sup>H NMR. The IR spectrum of PEG 1540 revealed peaks at 3440.1 cm<sup>-1</sup> (O–H stretch), 1286.5 cm<sup>-1</sup> (O–H deflection), 2857.0 cm<sup>-1</sup> (C–H stretch), 1251.7 cm<sup>-1</sup> (C–O deflection), 1110.6 cm<sup>-1</sup> (strong peak of C–O stretch of ether), and so forth. The second step in the synthesis of PEG bis amine was conversion of CH<sub>3</sub>SO<sub>2</sub>-PEG-SO<sub>2</sub>CH<sub>3</sub> to H<sub>2</sub>N-PEG-NH<sub>2</sub>, where one of the important peaks obtained was at 3145.8 cm<sup>-1</sup> (N–H stretch antisymmetric of substituted primary amine). <sup>1</sup>H NMR (CDCl<sub>3</sub>)  $\delta$  (ppm): 3.91 (t, 4H, NH<sub>2</sub>CH<sub>2</sub>CH<sub>2</sub>), 3.14 (t, 4H, NH<sub>2</sub>CH<sub>2</sub>), which were not found in the <sup>1</sup>H NMR of PEG 1540.

NHS ester of folic acid (Scheme 2) was synthesized using DCC and NHS following by a reported method.<sup>18</sup> The NHS ester of folic acid was characterized through IR spectroscopy. Important peaks obtained for the folic acid were at 1660.8 cm<sup>-1</sup> (aromatic C=C bending and stretching), 1487.9 cm<sup>-1</sup> (CH–NH–C=O amides bending), 828.4 cm<sup>-1</sup> (aromatic C–H bending and benzene 1,4-disubstitution), and for the NHS conjugated folic acid 3689.9 cm<sup>-1</sup> (amide N–H and C=O stretching), 3001.5 cm<sup>-1</sup> (carboxylic acid C=O and O–H stretching unconjugated), 1711.6 cm<sup>-1</sup> (ketones C=O unconjugated stretch), which confirmed the synthesis of NHS ester of folic acid. This NHS activated folic acid was conjugated to PEG bis amine (NH<sub>2</sub>-PEG 1540-NH<sub>2</sub>). The general strategy of

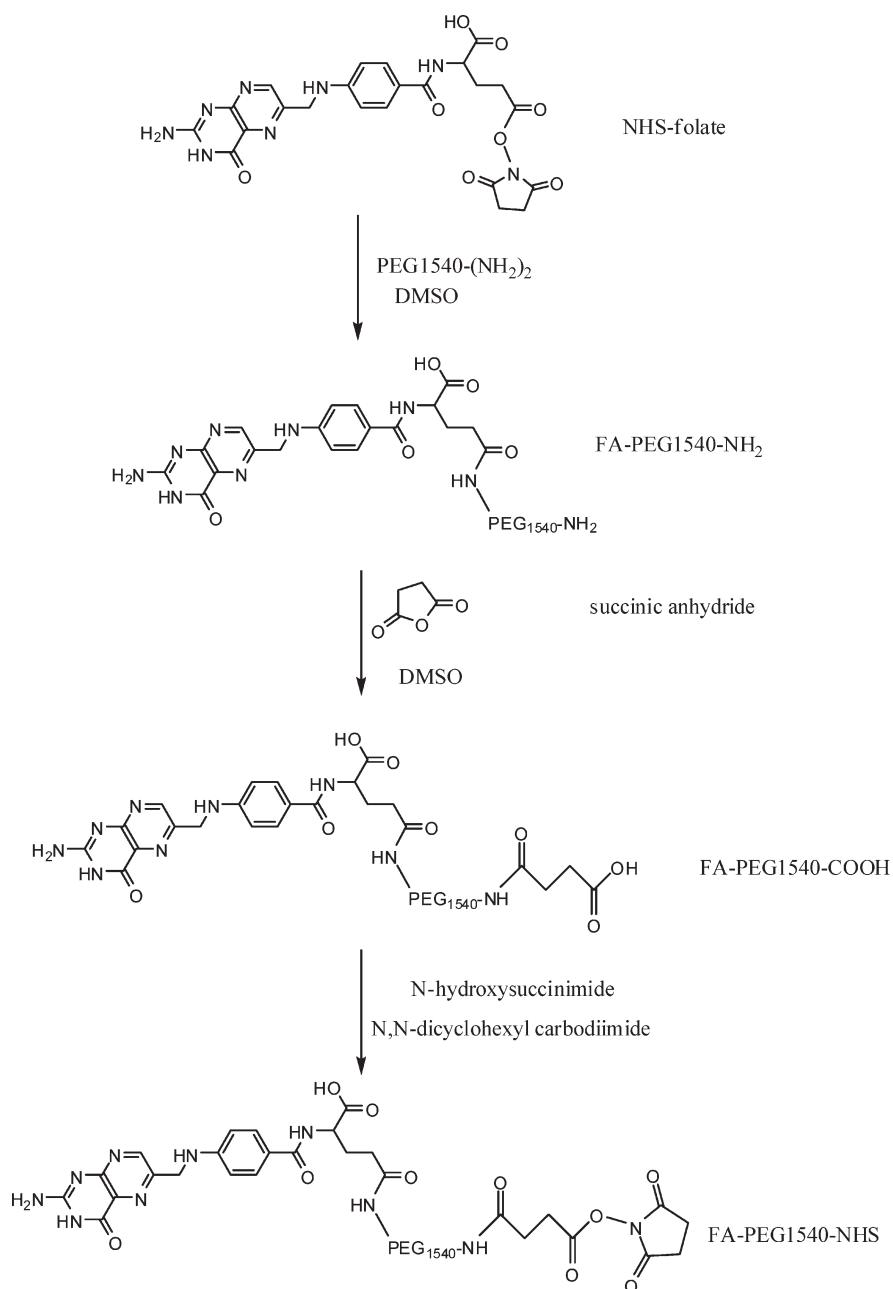
**Scheme 2.** Preparation of NHS Ester from Folic Acid<sup>a</sup>

<sup>a</sup> Reagents and conditions: DCC, NHS, DMSO, rt, 12 h.

the synthesis was shown in Scheme 3. H<sub>2</sub>N-PEG-FA was synthesized as previously described for the synthesis of NHS folate ester. The conjugation of folic acid to the unprotected primary amine of PEG was a complicated process. The byproduct of H<sub>2</sub>N-PEG-FA was accompanied with FA-PEG-FA due to no selectivity of the primary amine group in H<sub>2</sub>N-PEG-NH<sub>2</sub>. Additionally unreacted folic acid and H<sub>2</sub>N-PEG-NH<sub>2</sub> interfered with the purity of H<sub>2</sub>N-PEG-FA. Because of the ionic difference of these molecules, we decided to adopt Sephadex G-25 column for separation. The purity (> 95%) was confirmed by analytical HPLC (data not shown). ESI mass spectroscopic techniques further confirmed the conjugation of folic acid to the unprotected primary amine of PEG. Compared to that of H<sub>2</sub>N-PEG-NH<sub>2</sub>, the molecular weight of H<sub>2</sub>N-PEG-FA increased about 400–500, which indicated only one folic acid molecular conjugated to the H<sub>2</sub>N-PEG-NH<sub>2</sub>. Next, H<sub>2</sub>N-PEG-FA reacted with succinic anhydride, and to control the process more easy, the mount of succinic anhydride was 5-fold excess of H<sub>2</sub>N-PEG-FA. The side product was separated by washing with acetone. The FA-PEG-COOH was characterized through UV, IR spectroscopy, and <sup>1</sup>H NMR. In UV spectra, the peak at 282 nm indicates the presence of molecular folic acid. Important peaks obtained for the folic acid were at 1657.8 cm<sup>-1</sup> (aromatic C=C bending and stretching), 1477.2 cm<sup>-1</sup> (CH–NH–C=O amides bending), 836.4 cm<sup>-1</sup> (aromatic C–H bending and benzene 1,4-disubstitution). The <sup>1</sup>H NMR spectra confirmed the conjugation of the aromatic protons of folic acid (6.65, 7.55, and 8.66 ppm) and the multiplets of PEG (O–CH<sub>2</sub>–) at 3.6 ppm.

The active ester NHS-PEG1540-FA was obtained from FA-PEG-COOH in a similar manner to synthesis of FA-NHS in an earlier step. The NHS ester of PEG1540-FA was characterized through IR spectroscopy. Important peaks obtained for the NHS conjugated PEG-FA: 2930.8 cm<sup>-1</sup> (carboxylic acid C=O and O–H stretching unconjugated), 1699.6 cm<sup>-1</sup> (ketones C=O unconjugated stretch), which confirmed the synthesis of NHS ester of folic acid. <sup>1</sup>H NMR (CDCl<sub>3</sub>, 500 MHz): folic acid 8.64 (1H), 7.62 (2H), 6.68 (2H), 4.31 (2H); PEG 3.50 (140H); NHS 2.54 (4H); all of them confirmed the successfully syntheses of NHS ester of PEG-FA.

To increase the solubility and decrease the nonspecific cellular uptake, the primary amine on the surface of PAMAM dendrimer were partially converted to acetamide moieties in the presence of acetic anhydride and triethylamine (Figure 1).

**Scheme 3.** Synthesis of NHS-PEG1540–Folic Acid Conjugate from NHS–Folate<sup>a</sup>

<sup>a</sup> Reagents and conditions: (a) DMSO, 0 °C–rt, 12 h; (b) succinic anhydride, pyridine, DMSO, rt, 12 h; (c) DCC, NHS, DMSO, 0 °C–rt, 12 h.

The degree of acetylation was measured by <sup>1</sup>H NMR. <sup>1</sup>H NMR spectrum of the acetylated dendrimer showed the proton signal at δ 2.35 ppm, which corresponded to the methylene protons of –CH<sub>2</sub>C(O)– in dendrimer PAMAM G5. The specific signal at δ 1.93 ppm corresponded to the methyl protons of induced acetyl groups. The integration ratio of these two kinds of proton signals in the acetylated dendrimer suggested that an average of 77 acetyl groups are present on the surface of each G5 PAMAM dendrimer (Ac77-G5). There is a little difference with the reported method due to reaction conditions, especially temperature.<sup>26</sup> Conjugation of FA to the partially acetylated dendrimers was carried out via condensation between the γ-carboxyl group of FA and the primary amine of the dendrimer. The active ester of FA, formed by reaction with EDC in DMSO–DMF (1:3, volume ratio), was added dropwise to a solution of DI water containing G5-Ac

(77) and vigorously stirred for 3 days to confirm the reaction of FA and the G5-Ac (77) completes. The number of FA molecules attached to one dendrimer G5-Ac (77) was determined also by <sup>1</sup>H NMR.<sup>10,11,26</sup> The aromatic folate proton peaks could be observed at 6.83, 7.74, and 8.73 ppm. From the integral ratio of the folate proton at 8.73 ppm to the methylene protons of –CH<sub>2</sub>C(O)– in dendrimer PAMAM G5, approximately 4.5 folic acid molecular were found attached to each molecule of PAMAM dendrimer. UV spectroscopy, utilizing the free folic acid concentration calibration curve, determined the number of folic acid molecules to be 4.9.<sup>42</sup> By the other method, attachment of folic acid was accomplished through use of a PEG spacer. In the <sup>1</sup>H NMR spectrum of the conjugates, the aromatic folate proton peaks could be observed at 6.87, 7.73, and 8.78 ppm, along with PEG protons at 3.64 ppm. The multiple proton peaks from PAMAM were

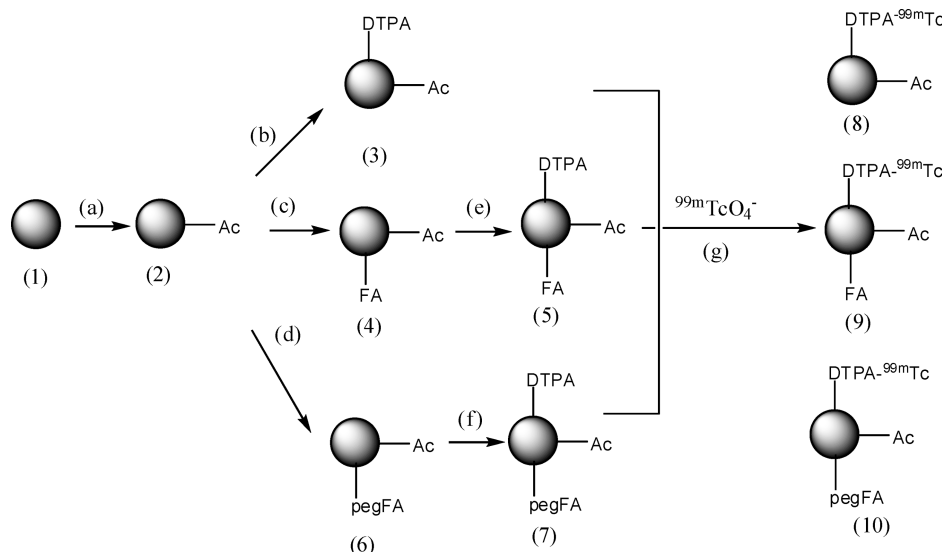


**Figure 1.** Synthetic procedure for multifunctional PAMAM dendrimer conjugates. Reagents and conditions: (a)  $\text{Ac}_2\text{O}$ ,  $\text{Et}_3\text{N}$ , 18 h, rt; (b) 1B4M-DTPA, pH = 9–10, 40 °C water; (c) FA, EDC, DMF/DMSO = 3:1; (d) FA-PEG-NHS, DMSO; (e) 1B4M-DTPA, pH = 9–10, 40 °C water; (f) 1B4M-DTPA, pH = 9–10, 40 °C water; (g)  $\text{Sn}^{2+}$ ,  $^{99m}\text{TcO}_4^-$ .

found between 2.4 and 3.7 ppm. From the integral ratio of the folate proton at 8.63 ppm to the multiplets of PAMAM, approximately 5.1 folate-PEG moieties were found attached to each molecule of PAMAM dendrimer. The number of FA molecules (5.2) was also determined by UV spectroscopy. For detecting the conjugates in live animals, we employed  $^{99m}\text{Tc}$  as radioactive nuclide, which is commercially available and easy to coordinate with bifunctional chelating agent DTPA. The partially acetylated dendrimer was reacted with 1B4M-DTPA, whereas isothiocyanates are active enough to react very easily with terminated primary amine of PAMAM, and the degree of functionalization can be controlled by stoichiometric control of reagents ratio and determined by a similar manner above ( $^1\text{H}$  NMR). In summary, each Ac-G5-DTPA contained 77 acetyl and eight DTPA molecules, Ac-G5-FA-DTPA contained 77 acetyl, 4.8 folic acid molecules, and seven DTPA molecules, and Ac-G5-pegFA-DTPA contained 77 acetyl, 5.2 folic acid molecules, and eight DTPA molecules. So three compounds (Ac-G5-pegFA-DTPA, Ac-G5-FA-DTPA, and Ac-G5-DTPA) contained the similar number (7–8) of DTPA molecules. Ac-G5-pegFA-DTPA and Ac-G5-FA-DTPA contained the similar number (4.8–5.2) of folic acid molecules.

**Radiochemistry.** All of the conjugates gave excellent radiochemical yield (above 95%), which can be used directly without further purification (Figure 2). A high-performance liquid chromatograph, equipped with a radioactivity  $\gamma$  detector, was used to monitor the conversion. The HPLC chromatograms in Figure 2 show that  $^{99m}\text{Tc}$ -G5-Ac-pegFA-DTPA (compound 10) had a retention time of 26.54 min, the  $^{99m}\text{Tc}$ -G5-Ac-FA-DTPA (compound 9) had a retention time of 12.36 min, and the  $^{99m}\text{Tc}$ -G5-Ac-DTPA (compound 8) had a retention time of 11.78 min. The mean recovery of five determinations of radioactivity was  $88.3\% \pm 1.0$ . It was because the nuclides decay and there were inevitable losses.

**In Vitro/in Vivo Stability Studies and Partition Coefficients.** The in vitro stability in PBS and new-born calf serum was studied (Table 1). The radioactive conjugates for all of the radiolabeled compounds keeps excellent in vitro stability in PBS and newborn calf serum at 37 °C within 6 h, and at least 86% and 84% conjugate still keeps the original structure,

respectively. In vivo, at least 80% of conjugate keeps good stability within 6 h in the blood of normal mice for all of the three conjugates.

Partition coefficients of the radiolabeled conjugates were determined by the ratio between *n*-octanol and water. The partition ratio of the three compounds: for compound 8 the Log *P* is  $-2.167$ , for compound 9 the Log *P* is  $-2.030$ , and for compound 10 the Log *P* is  $-2.061$ . The property of excellent water solubility further improves the radiolabeled yield. Octanol/water partition has a direct relationship with radiochemical yield and in vivo distribution. Similar lipid-water partition coefficient for studying whether folic acid played a target role is a more objective tool.

**Blood Clearance and Internalization.** We next evaluated the pharmacokinetic blood clearance of the three labeled compounds. Thus, the normal healthy mice received an intravenous dose of 0.74 MBq of the radiolabeled compounds, and blood samples were collected at various time intervals thereafter. As shown in Figure 3,  $^{99m}\text{Tc}$ -G5-Ac-pegFA-DTPA,  $^{99m}\text{Tc}$ -G5-Ac-FA-DTPA, and  $^{99m}\text{Tc}$ -G5-Ac-DTPA were rapidly removed from circulation in the mouse. The plasma half-life of the radiolabeled conjugates were estimated to be 13.15 min for  $^{99m}\text{Tc}$ -G5-Ac-pegFA-DTPA, 13.75 min for  $^{99m}\text{Tc}$ -G5-Ac-FA-DTPA, and 12.73 min for  $^{99m}\text{Tc}$ -G5-Ac-FA-DTPA, and less than 10% of the injected  $^{99m}\text{Tc}$  dose remained in circulation after 6 h (assuming that blood represents 5.5% of the total body mass). These data indicate that dendrimers conjugates are rapidly removed from circulation following intravenous administration and that valuable tissue biodistribution data can be obtained after only a few hours postinjection without the concern for nonspecific tissue uptake due to bloodborne radioactivity.

Cell uptake of  $^{99m}\text{Tc}$  labeled compounds was quantitatively measured, as shown in Figure 4. In the KB cell that express high levels of FR, in vitro cell binding of  $^{99m}\text{Tc}$ -G5-Ac-pegFA-DTPA was approximately 15% cell binding of total added radioactivity after incubation for 6 h at 37 °C. At the same time, the cell binding of  $^{99m}\text{Tc}$ -G5-Ac-FA-DTPA and  $^{99m}\text{Tc}$ -G5-Ac-DTPA were almost 11% and 10%, respectively. The data

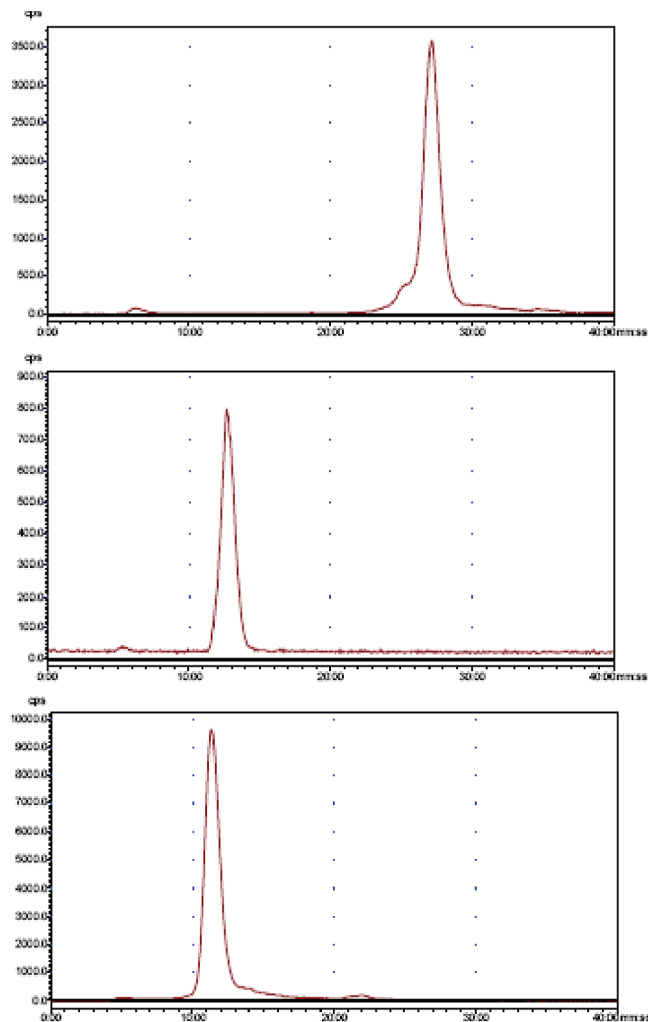


**Figure 2.** High performance liquid chromatography (HPLC) analyses of the complex (radioactivity  $\gamma$  detector): (upper)  $^{99m}\text{Tc}$ -G5-Ac-pegFA-DTPA, (middle)  $^{99m}\text{Tc}$ -G5-Ac-FA-DTPA, (lower)  $^{99m}\text{Tc}$ -G5-Ac-DTPA.

**Table 1.** In Vitro and in Vivo Stability of the Conjugate at 6 h after Injecting, Detected by RP-HPLC

6 h	PBS, %	serum, %	in vivo, %
8	87.41	84.69	80.56
9	86.33	85.24	80.45
10	86.26	85.14	80.78

indicated that  $^{99m}\text{Tc}$ -G5-Ac-DTPA and  $^{99m}\text{Tc}$ -G5-Ac-FA-DTPA exhibited a similar ability of internalization in FR-positive KB cells, improving only less than 1%. The data estimated conjugation of folic acid directly to 5.0 G PAMAM dendrimers almost could not improve cell uptake evidently. However,  $^{99m}\text{Tc}$ -G5-Ac-pegFA-DTPA, in which the PAMAM dendrimers conjugated to folic acid through the PEG linker, have higher KB cell uptake than non-PEG linker ( $^{99m}\text{Tc}$ -G5-Ac-DTPA). Results indicated that indirect folic acid conjugation through PEG spacer could improve the ability of folic acid by combining with folate receptor in the KB cancer cells. The uptake of three compounds in the KB cell that express low levels of FR was similar (< 10%), not showing any significant binding.

**In Vivo Biodistribution.** The ability of  $^{99m}\text{Tc}$ -dendrimers conjugations to target tumors in vivo was assessed by injecting BALB/c nude mice with KB cancer cells. The mice were

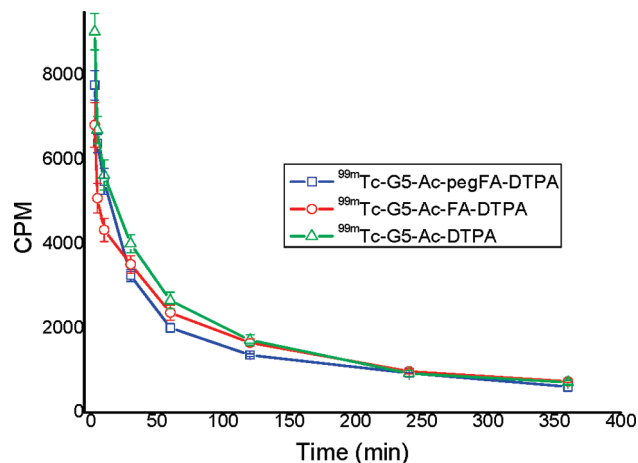


**Figure 3.** The concentration–time curve of  $^{99m}\text{Tc}$ -G5-Ac-pegFA-DTPA,  $^{99m}\text{Tc}$ -G5-Ac-FA-DTPA, and  $^{99m}\text{Tc}$ -G5-Ac-DTPA in normal mice. Each animal received an intravenous dose of 0.74 MBq. At the designated times postinjection, each animal was euthanized and blood was collected and counted for associated radioactivity. (Error bars:  $n = 3$  animals).

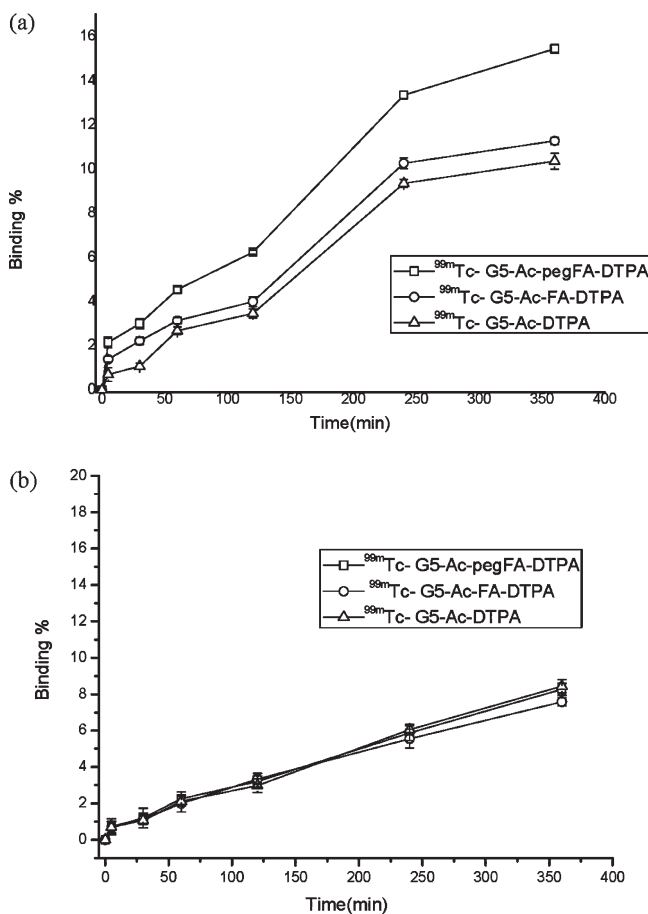


**Figure 4.** Time-dependent association of  $^{99m}\text{Tc}$ -G5-Ac-pegFA-DTPA,  $^{99m}\text{Tc}$ -G5-Ac-FA-DTPA, and  $^{99m}\text{Tc}$ -G5-Ac-DTPA. KB cells were incubated with 0.037 MBq  $^{99m}\text{Tc}$ -G5-Ac-pegFA-DTPA,  $^{99m}\text{Tc}$ -G5-Ac-FA-DTPA and  $^{99m}\text{Tc}$ -G5-Ac-DTPA for increasing periods of time at 37 °C. Following multiple washes, cells were harvested and counted for associated radioactivity. (a) KB cell that that express high levels of FR; (b) KB cell that that express low levels of FR (error bars:  $n = 3$ ).

maintained on a folate-deficient diet for the duration of the experiment to minimize the circulating levels of folic acid.

**Table 2.** In Vivo Biodistribution Analyses of  $^{99m}\text{Tc}$ -G5-Ac-pegFA-DTPA (**10**),  $^{99m}\text{Tc}$ -G5-Ac-FA-DTPA (**9**), and  $^{99m}\text{Tc}$ -G5-Ac-DTPA (**8**) in KB-Bearing Nude Mice Which Was Injected via the Tail Vein with 0.74 Mbq of  $^{99m}\text{Tc}$ -G5-Ac-pegFA-DTPA,  $^{99m}\text{Tc}$ -G5-Ac-FA-DTPA, and  $^{99m}\text{Tc}$ -G5-Ac-DTPA in 0.1 mL of Saline<sup>a</sup>

organ/tissue	$^{99m}\text{Tc}$ -G5-Ac-pegFA-DTPA			$^{99m}\text{Tc}$ -G5-Ac-FA-DTPA			$^{99m}\text{Tc}$ -G5-Ac-DTPA		
	2 h	4 h	6 h	2 h	4 h	6 h	2 h	4 h	6 h
blood	11.52(0.76)	6.81(0.83)	4.37(0.17)	12.59(0.59)	6.12(0.82)	4.00(0.25)	11.75(0.52)	7.38(0.64)	5.60(0.31)
muscle	0.96(0.12)	0.85(0.15)	0.66(0.14)	0.92(0.16)	0.90(0.18)	0.95(0.16)	1.07(0.31)	0.94(0.33)	0.78(0.25)
lungs	8.12(0.69)	6.27(0.40)	3.81(0.60)	5.96(0.70)	3.99(0.63)	2.77(0.57)	5.42(0.22)	3.30(0.58)	3.24(0.34)
liver	28.93(1.78)	26.29(1.33)	22.23(1.59)	32.02(0.82)	29.60(0.94)	26.17(1.41)	41.07(0.56)	37.19(1.41)	32.94(0.78)
kidney	18.21(0.67)	27.31(0.68)	28.82(0.94)	22.06(0.45)	24.85(0.80)	28.18(1.23)	32.08(0.74)	27.19(0.98)	26.06(0.79)
spleen	9.26(0.86)	10.82(0.95)	9.24(0.72)	7.55(0.65)	6.17(0.51)	5.49(0.59)	13.77(0.95)	11.88(0.81)	9.78(0.31)
heart	4.22(0.61)	2.43(0.45)	1.87(0.20)	2.89(0.18)	2.38(0.12)	2.02(0.17)	3.12(0.55)	2.57(0.25)	2.53(0.29)
stomach	3.17(0.29)	2.93(0.26)	2.11(0.26)	3.02(0.69)	3.14(0.20)	2.39(0.51)	2.17(0.29)	1.73(0.14)	1.86(0.46)
intestine	2.75(0.52)	2.58(0.30)	2.49(0.28)	1.28(0.43)	1.11(0.18)	0.95(0.29)	2.55(0.39)	2.22(0.47)	2.22(0.47)
brain	0.40(0.13)	0.32(0.07)	0.27(0.07)	0.53(0.17)	0.24(0.08)	0.21(0.09)	0.66(0.14)	0.50(0.08)	0.48(0.16)
bone	1.06(0.23)	0.93(0.19)	0.67(0.22)	0.90(0.19)	0.98(0.25)	1.25(0.35)	0.62(0.14)	0.41(0.15)	0.45(0.21)
skin	0.87(0.11)	0.70(0.12)	0.58(0.15)	0.93(0.24)	1.33(0.23)	1.17(0.19)	1.63(0.23)	1.20(0.22)	0.95(0.14)
tumor	3.82(0.19)	7.58(0.54)	10.27(0.59)	3.10(0.32)	5.89(0.32)	6.78(0.34)	2.81(0.45)	3.94(0.42)	4.38(0.38)

<sup>a</sup> Values expressed as percentage of injected dose per gram of tissue (%ID/g  $\pm$  SD),  $n = 3$ .

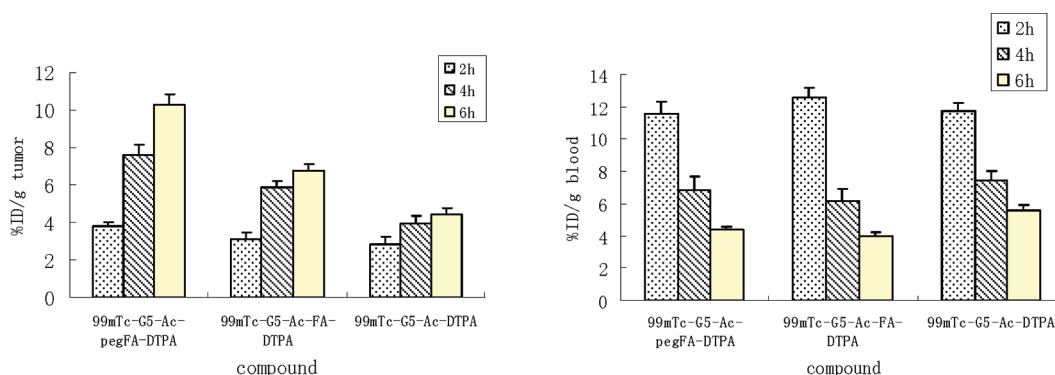


**Figure 5.** The uptake of  $^{99m}\text{Tc}$ -G5-Ac-pegFA-DTPA,  $^{99m}\text{Tc}$ -G5-Ac-FA-DTPA, and  $^{99m}\text{Tc}$ -G5-Ac-DTPA in tumor and blood.

After receiving the same dose of labeled compounds, animals were euthanized at the designated times and selected tissues were removed, weighed, and counted to determine  $^{99m}\text{Tc}$  distribution. Table 2 summarizes the results of biodistribution studies in KB-bearing nude mice at 2, 4, and 6 h post intravenous injection of the three  $^{99m}\text{Tc}$  labeled compounds (Figure 5). We first examined the biodistribution and elimination of  $^{99m}\text{Tc}$ -G5-Ac-pegFA-DTPA to test its ability to target the folate receptor-positive human KB tumor xenografts established in immunodeficient nude mice. The conjugates were cleared rapidly from the blood, decreased from 11.52% ID/g at 2 h to 4.37% ID/g at 6 h. In several other organs, such as lungs, heart, stomach, and intestine, the uptake of the conjugated kept at a low level. These organs are known not to express folate receptor and do not show significant differences between the nontargeted and the targeted dendrimers.  $^{99m}\text{Tc}$ -G5-Ac-DTPA and  $^{99m}\text{Tc}$ -G5-Ac-FA-DTPA show the similar uptake in these organs. The concentrations of the three conjugates in the brain were low at all time points, suggesting that the dendrimer conjugates could not cross the blood–brain barrier. The same results were shown in the muscle, bone, and skin, which were further confirmed by the micro-SPECT imaging. The kidneys are the major clearance organs for the dendrimers, and they are known to express high levels of the folate receptor on its tubules.<sup>43–46</sup> The level of nontargeted  $^{99m}\text{Tc}$ -G5-Ac-DTPA decreased from 32.08% ID/g at 2 h to 26.06% ID/g at 6 h. In contrast, the level of  $^{99m}\text{Tc}$ -G5-Ac-FA-DTPA and  $^{99m}\text{Tc}$ -G5-Ac-pegFA-DTPA increased slightly with time due to

folate receptors present on the kidney tubules. The liver and KB tumor cells are known to express high levels of folate receptor. In the liver, the concentrations of nontargeted  $^{99m}\text{Tc}$ -G5-Ac-DTPA decreased with the clearance of the dendrimer from the blood. In contrast, the targeted  $^{99m}\text{Tc}$ -G5-Ac-FA-DTPA and  $^{99m}\text{Tc}$ -G5-Ac-pegFA-DTPA decreased much more slowly. In tumor cells, the level of  $^{99m}\text{Tc}$ -G5-Ac-pegFA-DTPA increased from 3.82% ID/g at 2 h to 10.27% ID/g at 6 h. The level of  $^{99m}\text{Tc}$ -G5-Ac-FA-DTPA increased from 3.10% ID/g at 2 h to 6.78% ID/g at 6 h. The nontargeted  $^{99m}\text{Tc}$ -G5-Ac-DTPA also increased slightly from 2.81% ID/g at 2 h to 4.38% ID/g at 6 h. From Table 2 we could see this is extremely similar for their distribution in the live animals, and it is because the structure of the three compounds are similar. Only for those organs that contain folate receptors does their distribution have some differences. Compared with the results reported in the literature using  $^3\text{H}$  labeled dendrimer–folate conjugates, our conjugates will find wide application in micro-SPECT imaging study.

**Micro-SPECT Imaging.** The predominant uptake of  $^{99m}\text{Tc}$ -dendrimers conjugations by the FR-positive tumors, liver, and kidneys was further demonstrated by micro-SPECT imaging. As shown in Figure 6, a ventral image taken of a mouse 4 h after receiving 18.5 MBq dose of  $^{99m}\text{Tc}$ -dendrimers conjugations distinctively localizes the  $\gamma$  radiation to the kidneys, liver, and the tumor mass. No appreciable radiotracer was observed in the other tissues.

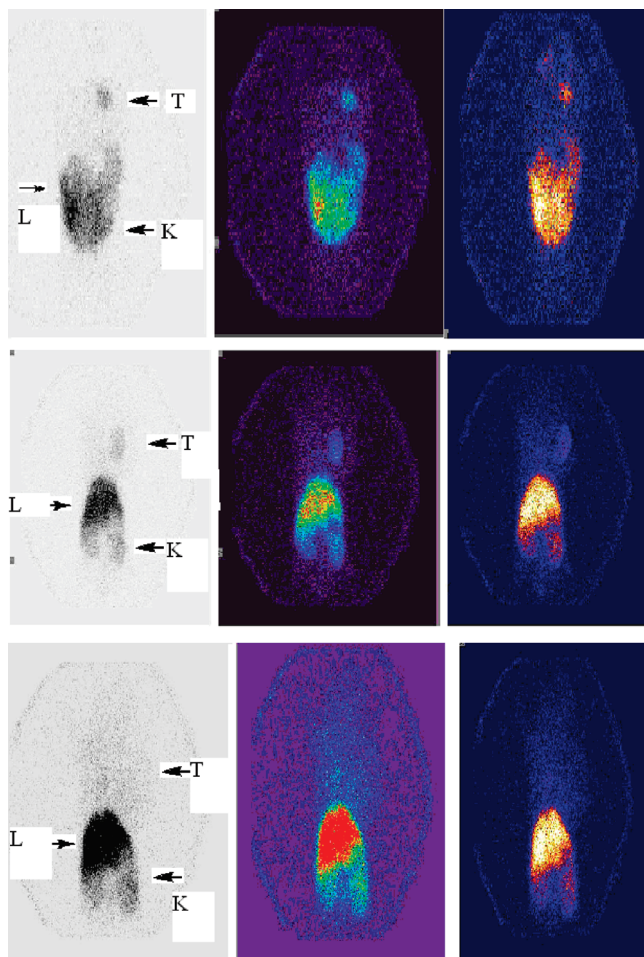


**Figure 6.** micro-SPECT images of KB-bearing nude mice at 4 h: T, tumor; L, lungs; K, kidney ((upper)  $^{99m}\text{Tc}$ -G5-Ac-pegFA-DTPA, (middle)  $^{99m}\text{Tc}$ -G5-Ac-FA-DTPA, (lower)  $^{99m}\text{Tc}$ -G5-Ac-DTPA).

## Discussion

The primary goal of this investigation was to identify a dendrimer-based  $^{99m}\text{Tc}$ -folate conjugate candidate for micro-SPECT imaging study. This project required the design, synthesis, analytical, and radiochemical characterization of a new chemical entity as well as *in vitro* and *in vivo* biological evaluations. Generation five (G5) PAMAM dendrimer, the well-defined structure and composition, as well as the narrow polydispersity of dendrimers, lead to their extensive applications for targeted cancer therapeutics. However, dendrimer-based therapeutics (fluorescein labeled) does not allow the direct imaging in live animals because of their weak signal strength. One major advantage of using  $^{99m}\text{Tc}$  is the visual imaging of small animals in which folic acid was chosen as the targeting agent. Folic acid is an essential precursor for the synthesis of nucleic acids and some amino acids, which is not produced endogenously by mammalian cells and requires internalization by cells via either receptor-mediated endocytosis or a carrier-based uptake mechanism. Compared with other targeted market such as monoclonal antibody and RGD peptides, folic acid has lower immunogenicity and relatively simpler chemistry. The folic acid receptor (FR) based mechanism constitutes a particularly useful target for tumor-specific drug delivery because it is upregulated in many human cancers, including malignancies of the ovary, brain, kidney, breast, and lung. The FR density also appears to

increase as the stage/grade of the cancer increases. The folate receptor has a high affinity for folic acid ( $K_d \sim 0.1 \text{ nM}$ ),<sup>47–51</sup> so this vitamin was worthy of attention as a targeting ligand for metastatic tumors through the lymphatic system. The most efficient method for assessing whether normal cells might bind and internalize folate conjugates was to examine the biodistribution of radiolabeled folate-linked imaging agent. Several folate-based  $^{99m}\text{Tc}$  conjugates without dendrimer PAMAM have previously been described in the literature<sup>37,39,48</sup> in which it is difficult for synthesis and purification. In our research, the chemical synthesis is relatively simple and the radiolabeled conjugates do not need to be purified before further evaluation due to its excellent radiochemical yield.

In this paper, we prepared three radiolabeled dendrimer conjugates of similar structure, i.e., G5-Ac-DTPA, G5-Ac-FA-DTPA, and G5-Ac-pegFA-DTPA. The choice of PEG as spacer was based on the following reason: PEG is hydrophilic and structurally flexible, potentially evading the recognition and phagocytosis by macrophage cells in the lymphatic system. This enables folic acid modified with PEG to selectively bind with a metastatic tumor-cell leading to receptor-mediated endocytosis. In this paper, we first prepared three Tc-99m labeled dendrimer folic acid conjugates in which it was determined that the folate receptors mediated endocytosis *in vitro*. Our results from *in vitro* cell uptake investigation demonstrated the receptor-mediated endocytosis properties of the folate conjugate with PAMAM dendrimer backbone. Compared with PEGylated dendrimer folic acid conjugate, the PEG unmodified conjugate reveals a low chance for the receptor binding. The biodistribution study further demonstrated the dendrimer folic acid conjugate through PEG linker had higher uptake in tumor. All of the  $^{99m}\text{Tc}$ -dendrimer conjugates show excellent *in vitro* stability in PBS and serum within 360 min. More than 75% of the conjugate keeps its original structure in mice for all of the three conjugates within 360 min.

A new report from the nation's leading cancer organizations (NCI: National Cancer Institute) shows that, in 2009, 1479350 people were diagnosed with cancer and 562340 people died of cancer in the United States. One reason for the low survival rate is the difficulty in diagnosing cancer. Because  $^{99m}\text{Tc}$ -G5-Ac-pegFA-DTPA binds tightly to FR, which is present in large amounts on cancers, this radiopharmaceutical may provide an inexpensive, noninvasive, but reliable method for the early diagnosis of cancer. In our research, a new dendrimer derivative of folic acid was created to efficiently chelate Tc-99m. This new compound,  $^{99m}\text{Tc}$ -G5-Ac-pegFA-DTPA, avidly binds to FR-positive tumor cells *in vitro* and *in vivo*. These results indicate that this new compound merits further investigation as a noninvasive radioactive diagnostic imaging agent for the detection of FR-positive cancers. Our group recently reported a similar compound "G5-Ac-FA-DTPA<sub>15</sub>", with only the number of DTPA molecules increased. The uptake at 6 h in livers and kidneys changed very much (livers:  $5.71 \pm 0.41\% \text{ ID/g}$  vs  $26.17 \pm 1.41\% \text{ ID/g}$ ; kidneys:  $40.43 \pm 2.64\% \text{ ID/g}$  vs  $28.18 \pm 1.23\% \text{ ID/g}$ ). Therefore, we believed that the number of carboxyl and amino groups in the surface of dendrimers played an important role in targeting. How to find the best ratio of the two groups is under investigation in our group.

## Conclusion

We have synthesized and radiolabeled three dendrimer PAMAM folic acid conjugates which keep excellent *in vitro/in vivo*

stability and rapid clearance from blood. Biodistribution study of KB tumor bearing nude mice showed specific accumulation was observed in tumors, which was further confirmed by micro-SPECT imaging study. Our results demonstrated that indirect folic acid conjugation through PEG spacer increased the uptake in tumors and the potential of folic acid conjugated dendrimer as a promising imaging tool for cancer diagnosis.

## Experimental Section

**Materials.** PAMAM dendrimer generation 5 (G5-NH<sub>2</sub>) were purchased from Aldrich Co., Ltd. *N*-Hydroxysuccinimide (NHS, 99%), *N,N*-dicyclohexyl carbodiimide (DCC, 98%), 1-[3-(dimethylamino)propyl]-3-ethylcarbodiimide HCl (EDC, 98%), and triethylamine, folic acid (FA) were purchased from Aldrich Co., Ltd. PEG1540, acetic anhydride, dimethyl sulfoxide (DMSO, 99%), dimethylformamide (DMF, 99%), and dialysis membrane (MWCO, 3500 and 14000) were purchased from Sinopharm Chemical Reagent Co., Ltd. (Shanghai). Carrier-free <sup>99m</sup>Tc-pertechnetate was freshly eluted with saline from <sup>99</sup>Mo/<sup>99m</sup>Tc-generator (Shanghai Yuanpu Isotope Technology Co., Ltd.). 2-(*p*-Isothiocyanatobenzyl)-6-methyl-diethylenetriaminopentaacetic acid (1B4M-DTPA) was a gift from Dr. Martin W. Brechbiel (NIH). All of the reagents were used as received without further purification. KB cells were purchased from Shanghai Institute of Biochemistry and Cell Biology, Chinese Academy of Sciences. BALB/c nude mice and Kunming mice was obtained from Shanghai Laboratory Animal Center, Chinese Academy of Sciences. <sup>1</sup>H NMR spectrum was performed on Bruker AVANCE DRX 500 spectrometer in D<sub>2</sub>O solution. ESI-MS was measured on a ThermoQuest Finnigan LCQ-Duo in the positive ion mode. Elution was in a mixture of 50:50 water:ACN at a flow rate of 0.2 mL/min. The micro-SPECT imaging system developed in our institute consists of a stationary mini  $\gamma$  camera with pinhole collimator or parallel collimator and vertical object rotation mechanism. The mini  $\gamma$  camera is based on a 5 mm thick pixellated NaI (TI) crystal array with 1.2 mm pixel size and 1.4 mm pixel pitch coupled to a 5 in. diameter Hamamatsu R3292 position sensitive photomultiplier tube (PSPMT). All of the conjugates (<sup>99m</sup>Tc-Ac-G5-pegFA-DTPA, <sup>99m</sup>Tc-Ac-G5-FA-DTPA, and <sup>99m</sup>Tc-Ac-G5-DTPA) gave excellent radiochemical purity (above 95%) determined by HPLC.

**Reverse Phase High Performance Liquid Chromatography.** A Phenomenex (Torrance, CA) Jupiter C5 silica-based HPLC column (250 mm  $\times$  4.6 mm, 300 Å) was used for the separation of analyt. Two Phenomenex Wdepore C5 guard columns (4 mm  $\times$  3 mm) were also installed upstream of the HPLC column. The mobile phase for elution of PAMAM dendrimers was a linear gradient beginning with 90:10 water/acetonitrile (ACN) at a flow rate of 1 mL/min, reaching 50:50 after 30 min. Trifluoroacetic acid (TFA) at 0.14 wt % concentration in water as well as in ACN was used as a counterion to make the dendrimer conjugate surfaces hydrophobic. The conjugates were dissolved in the mobile phase (90:10 water/ACN). The injection volume in each case was 100  $\mu$ L, with concentration of approximately 1 mg/mL. Contained radioactive outflow of fluid was collected in a sealed vial.

**Synthesis and Characterization of PEGylated Dendrimer Conjugates. Preparation of Diaminopolyoxyethylene1540.** First, 5 g (3.3 mmol) of dry poly(ethylene)glycol (PEG) 1540 was dissolved in 100 mL of dry CH<sub>2</sub>Cl<sub>2</sub>. Then 7 mL of triethylamine was added, the reaction was cooled in an ice-water bath, and 1 mL (13.3 mmol) of CH<sub>3</sub>SO<sub>2</sub>Cl was added dropwise with stirring. When all of the CH<sub>3</sub>SO<sub>2</sub>Cl was added, the ice bath was removed and the reaction was stirred overnight at room temperature. The reaction mixture was washed with 100 mL of 50 mM NaHCO<sub>3</sub>. The organic fraction was dried over MgSO<sub>4</sub> and filtered, and the solvent was evaporated to give dimethanesulfonylpolyoxyethylene1540 that was immediately dissolved in 150 mL of a concentrated solution of aqueous ammonia and was left to stir for

48 h in a sealed flask.<sup>19</sup> The product was extracted twice with CH<sub>2</sub>Cl<sub>2</sub>, the organic fractions were combined, dried over MgSO<sub>4</sub>, and filtered, and the solvent was removed under reduced pressure (Scheme 1). The product was crystallized from Et<sub>2</sub>O. The yield was 80%. <sup>1</sup>H NMR (CDCl<sub>3</sub>)  $\delta$  (ppm): 3.91 (t, 4H, NH<sub>2</sub>CH<sub>2</sub>CH<sub>2</sub>), 3.14 (t, 4H, NH<sub>2</sub>CH<sub>2</sub>), 3.66 (bs, ~136H, OCH<sub>2</sub>CH<sub>2</sub>O).

**Preparation of FA-NHS Ester.** Folic acid (600 mg, 1.34 mmol) was dissolved in 24 mL of dry DMSO to which 279 mg (1.00 mmol) of DCC and 154 mg (1.34 mmol) of NHS were added (Scheme 2). The reaction was left overnight at room temperature in the dark. The DCU precipitate (a side product of the reaction) was filtered out, and 150 mL of 30% acetone in Et<sub>2</sub>O was added with stirring. The yellow precipitate was collected on sintered glass and washed with acetone and ether and was used immediately in the next step.

**Preparation of NHS-Activated PEGylated Folic Acid.** First, 130 mg (296  $\mu$ mol) of FA-NHS ester was added to PEG-1540 bis-amine (900 mg, 450  $\mu$ mol) in DMSO (15.0 mL) solution in the presence of pyridine (15.0  $\mu$ L). Then the mixture was stirred overnight, and the product was purified by filtration over a Sephadex G-25 column equilibrated with 0.1 M NaHCO<sub>3</sub> to remove unconjugated folic acid and unreacted PEG-bis amine fragments. The filtrate obtained was precipitated with acetone and the solid collected was dried under vacuum, yielding pegylated folic acid (NH<sub>2</sub>-PEG-FA) as a pale-yellow solid. ESI mass spectroscopic techniques confirmed the conjugation of folic acid to the unprotected primary amine of PEG. Compared to that of H<sub>2</sub>N-PEG-NH<sub>2</sub>, the molecular weight of H<sub>2</sub>N-PEG-FA increased from 400 to 500, which indicated only one folic acid molecular conjugated to the H<sub>2</sub>N-PEG-NH<sub>2</sub>. Thereafter, 50 mg of the above product was dissolved in DMSO (5.0 mL) containing pyridine (5.0  $\mu$ L) as a base, and a 5-fold excess of succinic anhydride was added. After stirring overnight, the PEG was precipitated by addition of acetone. The product was redissolved in DCM and filtered, and solvents were removed under reduced pressure. FA-PEG1540-COOH was obtained, which was characterized by UV, IR spectroscopy, and <sup>1</sup>H NMR. FA-PEG1540-NHS was prepared by the similar procedure used for the synthesis of the NHS ester of folic acid and was purified by chromatography on silica gel using CH<sub>2</sub>Cl<sub>2</sub>:methanol = 8:1. The product was characterized by UV, IR spectroscopy, and <sup>1</sup>H NMR.

**Dendrimer PAMAM Generation 5 (1).** PAMAM dendrimer generation 5 (G5) were purchased from Aldrich Co., Ltd. The surface group is -NH<sub>2</sub>, and the number average molecular weight were found to be 28824 g/mol.

**Acetylated Dendrimer PAMAM Generation 5 (Ac-G5) (2).** Partially acetylated PAMAM dendrimer generation 5 (Ac-G5) was performed according to the reported procedure.<sup>26</sup> Briefly, acetic anhydride (70% ratio of primary amine numbers of a G5 PAMAM dendrimer, 14.65  $\mu$ L) was slowly added to the dendrimer G5 solution (50 mg, 1.73  $\mu$ mol dendrimer G5 dissolved in 6 mL methanol) in the presence of triethylamine (1.25 equivalent of acetic anhydride, 27.00  $\mu$ L). The mixture was stirred under N<sub>2</sub> atmosphere at room temperature. After 18 h, methanol was evaporated on a rotary evaporator. The residue was dissolved in water and dialyzed (using cellulose membrane with 3500 MWCO) against PBS buffer and double distilled (DI) water for 3 days. The obtained sample Ac-G5 was lyophilized and stored in a dry place before further modification and characterization. Yield: 94.7%.

**Acetylated PAMAM-G5-DTPA Conjugate (Ac-G5-DTPA) (3).** The Ac-G5 (2) was concentrated to the concentration of 5 mg/mL and reacted with excess of 1B4M-DTPA (MW = 555 g/mol) at 40 °C, and the ratio of Ac-G5 to 1B4M-DTPA was 1:10 (molar ratio). The reaction mixture was maintained at pH = 9–10 during the reactive time of 36 h. The resulting mixture was purified by dialysis (using cellulose membrane with 14000 MWCO, PBS buffer, and DI water 3 times respectively with 1 L for each time) and lyophilization. The obtained compound is

conjugate Ac-G5-DTPA, which was lyophilized and stored in a dry place before further modification. Yield: 96.2%.

**Acetylated Dendrimer PAMAM Generation 5–Folic Acid Conjugate (Ac-G5-FA) (4).** First, 6.12 mg of folic acid (MW = 441.4 g/mol) reacted with 29.69 mg of EDC·HCl (MW = 191.71 g/mol, 14-fold of FA) in a mixture of 6 mL dry DMF and 2 mL dry DMSO for 1 h at room temperature. The reaction mixture was added dropwise to the DI water solution (15 mL) of 1.39  $\mu$ mol of Ac-G5 (The molar ratio of Ac-G5 to FA was 1:6) and vigorously stirred for 3 days at room temperature. After dialysis (using cellulose membrane with 3500 MWCO, PBS buffer and DI water 3 times with 1 L each time) and lyophilization, the yield was 94.5%. Further purification was carried out by membrane filtration with DI water. The obtained sample Ac-G5-FA was lyophilized and stored in a dry place before further modification. Yield: 90.8%.

**Acetylated PAMAM G 5–Folic Acid–DTPA Conjugate (Ac-G5-FA-DTPA) (5).** This compound was obtained in 97.4% yield on the basis of the similar procedures for preparing Ac-G5-DTPA (3). Ac-G5-FA reacted with 10-fold molar excess of 1B4M–DTPA.

**Indirect Folic Acid Conjugation through PEG Spacer (Ac-G5-pegFA) (6).** The mixture of active ester FA-PEG1540-NHS in DMSO (25 mg/mL) with the partially acetylated PAMAM dendrimer generation 5 (Ac-G5) in DMSO (10 mg/mL) was stirred for 5 days at room temperature (25 °C) using a metabolic shaker. The ratio of FA-PEG1540-NHS to Ac-G5 was 8:1 (molar ratio), after dialysis (using cellulose membrane with 3500 MWCO, PBS buffer and DI water 3 times with 1 L each time) and lyophilization to give almost pure compound, which was further purified by membrane filtration with DI water. The obtained sample Ac-G5-pegFA was lyophilized and stored in a dry place before further modification. Yield: 93.7%.

**Acetylated PAMAM G 5–(PEG Linker) Folic Acid–DTPA Conjugate (Ac-G5-pegFA-DTPA) (7).** This compound was obtained in 94.4% yield on the basis of the similar procedures for preparing Ac-G5-DTPA (3). Ac-G5-pegFA reacted with 10-fold molar excess of 1B4M–DTPA.

**Radiolabeling.** [ $^{99m}\text{Tc}$ ]sodium pertechnetate was eluted from a  $^{99m}\text{Tc}/^{99}\text{Mo}$  generator using 0.9% saline.  $\text{Na}[\text{}^{99m}\text{TcO}_4]$  (5 mCi in 1 mL of saline) was added to the shielded vial containing the Ac-G5-pegFA-DTPA solution (20 mg in 2 mL of helium-purged water, contained 0.1 mL 1 M of stannous chloride). The reaction vial was purged with nitrogen, shaken, and heated for 30 min in a water bath (80 °C) before analysis. The final reaction mixture was analyzed by RP-HPLC.<sup>38,39</sup> The similar procedure was applied to the  $^{99m}\text{Tc}$ -Ac-G5-FA-DTPA and  $^{99m}\text{Tc}$ -Ac-G5-DTPA.

**Evaluation of in Vitro/in Vivo Stability.** Stability of the synthetic complexes was studied by measuring the radiochemical purity using radio-HPLC (the conditions of the RP HPLC assay used to measure label stability were the same as described above) at different time intervals after preparation. The complex was added to a test tube containing PBS solution. The mixture was incubated by shaking at 37 °C in a Thermomixer. The radiochemical purity was measured at 30 min, 1 h, 2 h, 4 h and 6 h by radio-HPLC. The same procedure was applied to the experiment using newborn calf serum.

The in vivo stability was evaluated as followed, after preparation of the labeled compound, 1.85 MBq conjugate was withdrawn and 100  $\mu$ L of saline was added. Then the conjugate solution was injected into healthy Kunming mice (4 weeks old) via tail vein. Mice were euthanized and blood was removed quickly after certain times (15 min, 30 min, 1 h, 2 h, 4 h, 6 h) ( $n=3$  for all time points). HCl 0.1 mL (6 M) was added to the blood samples, which were centrifuged at 10000 rpm for 1 min at 20 °C, and the supernatant was collected in a test tube containing  $\text{CH}_3\text{CN}$  (500  $\mu$ L). After the tube was vortexed for 30 s and centrifuged at 10000 rpm for 5 min at 20 °C, the supernatant was withdrawn to measure the radiochemical purity by RP-HPLC.

**Measurement of the Octanol/Water Partition Coefficient.** Partition coefficients were measured according to Saji's method.<sup>40</sup>

A 10  $\mu$ L aliquot of aqueous solution of each labeled compound was mixed with 3 mL of *n*-octanol and 3 mL of phosphate buffer at pH = 7.4. The mixture was vigorously shaken for 3 min at room temperature using a vortex mixer, and the solution was then incubated for 30 min. This workup was conducted 3 times. The organic layer and the phosphate buffer solution were collected, and the radioactivity was measured with a  $\gamma$  counter.

**Cell Uptake.** The KB cell line is a human oral epidermoid carcinoma that overexpresses FR, especially when grown in a low folic acid medium. The KB cells were grown continuously as a monolayer at 37 °C and 5%  $\text{CO}_2$  in folic-acid-deficient RPMI 1640 medium containing 10% heat-inactivated fetal bovine serum (FBS), yielding a final folate concentration roughly that of normal human serum.<sup>25,41</sup> The cells grown in FA-free media express high-level FR, while the cells grown in FA-containing media express low-level FR. About  $1 \times 10^6$  cells per well were seeded in 24-well plates for 24 h before the in vitro targeting efficacy studies. The cells were then incubated with the conjugates (final concentrations of 0.037 MBq for  $^{99m}\text{Tc}$ -Ac-G5-pegFA-DTPA,  $^{99m}\text{Tc}$ -Ac-G5-FA-DTPA, and  $^{99m}\text{Tc}$ -Ac-G5-DTPA, about 0.001 mg substrates) and maintained at 37 °C for 30 min, 1 h, 2 h, 4 h, and 6 h. At the end of incubation period, the medium was moved, the cells were washed three times with 0.5 mL PBS buffer, the medium (including PBS buffer) and cells was collected, and the radioactivity was measured with a  $\gamma$  counter. The cell uptake was expressed as followed:

$$\text{cell uptake} = \frac{\text{cell radioactivity}}{\text{total radioactivity}} \times 100\%$$

**Pharmacokinetics and Biodistribution Studies.** The pharmacokinetics was determined in normal healthy Kunming mice (4 weeks old). Each animal received a dose of 0.74 MBq of the radiolabeled compounds in approximately 0.2 mL volume iv via the tail vein ( $n=5$ ). At the designated times (1, 5, 10, 15, 30, 60, 120, 240, 360 min), each animal's blood was immediately collected via the tail vein. The blood clearance curve for  $^{99m}\text{Tc}$ -G5-Ac-pegFA-DTPA,  $^{99m}\text{Tc}$ -G5-Ac-FA-DTPA, and  $^{99m}\text{Tc}$ -G5-Ac-DTPA in normal mice was detected in a  $\gamma$  counter. The  $\alpha_{1/2}$  and  $\beta_{1/2}$  were calculated using Drug and Statistics Software DAS 2.0 (Wuhu Gauss Data Analysis Ltd.) where  $C$  concentration is the amount of radioactivity per milligram (cpm/mg) in blood of normal mice.

The in vivo biodistribution of the radiolabeled compounds in KB-bearing nude mice was assessed by injecting BALB/c nude mice. Mice were housed under conditions of controlled temperature (26 °C), humidity (68%), and daily light cycle (12 h light/12 h dark). The mice were maintained on a folate-deficient rodent chow (in order to reduce their serum folate to a level near that of human serum). After an acclimation period of two weeks, BALB/c male nude mice were inoculated subcutaneously in the right flank with  $5 \times 10^6$  cultured human oral epidermoid carcinoma KB cells. Three weeks after the inoculation, when the tumor reached  $1 \times 1 \text{ cm}^2$ , the mice were injected with 0.74 MBq of activity in 100  $\mu$ L (contained 0.01 mg substrates) of saline through the tail vein ( $n=3$ , at all time points, for all of the three compounds). Mice were sacrificed at various time points (2, 4, and 6 h). Their organs were harvested and weighed, and their radioactivity was measured in a  $\gamma$  counter and counted to determine the percentage of activity incorporated into the tissues. Each time (data) point was carried out in quintuples. This was expressed as percentage of injected dose per gram of tissue (% ID/g  $\pm$  SD). The resultant data were expressed as mean values with standard deviations.

$$\text{organ uptake} = \frac{\text{organ radioactivity}}{\text{total radioactivity} \times \text{organ weight(g)}} \times 100\%$$

**Micro-SPECT Imaging.** For in vivo imaging, BALB/c male nude mice were inoculated subcutaneously in the right flank with  $2 \times 10^6$  cultured human oral epidermoid carcinoma KB

cells. When tumor size reached an average of 0.8 cm in diameter, mice were assigned in one of the three groups, with two mice in each group. Group 1 received  $^{99m}\text{Tc}$ -Ac-G5-pegFA-DTPA (18.5 MBq of Ac-G5-pegFA-DTPA, contained 0.25 mg substrates) through the tail vein, group 2 received  $^{99m}\text{Tc}$ -Ac-G5-FA-DTPA, and group 3 received  $^{99m}\text{Tc}$ -Ac-G5-DTPA. Five-minute planar static images in prone were acquired at 4 h after injection, using a  $\gamma$  camera equipped with a pinhole collimator.

**Acknowledgment.** We gratefully acknowledge Dr. Martin W. Brechbiel (NIH) for his kind donation of 1B4M-DTPA. Financial support is from the Chinese Academy of Sciences (Hundreds Talent Program 26200601), Natural Science Foundation of Shanghai (no. 3109ZR1438400), and the National Natural Science Foundation of China (no. 10905087).

## References

- Torchilin, V. P. Targeted pharmaceutical nanocarriers for cancer therapy and imaging. *AAPS J.* **2007**, *9*, E128–E147.
- Nazila, K.; Tammy, K.; Maya, T.; Jimmy, D. B.; Andrew, D. M. Folate Receptor Targeted Bimodal Liposomes for Tumor Magnetic Resonance Imaging. *Bioconjugate Chem.* **2009**, *20* (4), 648–655.
- Esfand, R.; Tomalia, D. A. Poly(amidoamine) (PAMAM) dendrimers: from biomimicry to drug delivery and biomedical applications. *Drug Discovery Today* **2001**, *6*, 427–436.
- Majoros, I. J.; Mehta, C. B.; Baker, J. R., Jr. Mathematical Description of Dendrimer Structure. *J. Comput. Theor. Nanosci.* **2004**, *1*, 193–198.
- Tomalia, D. A.; Majoros, I. J. Dendritic Supramolecular and Supramacromolecular Assemblies. In *Supramolecular Polymers*; Ciferri, A., Ed.; Marcel Dekker Inc.: New York, 2000; pp 359–434.
- Tomalia, D. A.; Baker, H.; Dewald, J.; Hall, M.; Kallos, G.; Martin, S.; Roeck, J.; Ryder, J.; Smith, P. A New Class of Polymers: Starburst-Dendritic Macromolecules. *Polym. J.* **1985**, *17*, 117–132.
- Tomalia, D. A. Birth of a new macromolecular architecture: dendrimers as quantized building blocks for nanoscale synthetic polymer chemistry. *Prog. Polym. Sci.* **2005**, *30*, 294–324.
- Majoros, I. J.; Myc, A.; Thomas, T. P.; Mehta, C. B.; Baker, J. R., Jr. PAMAM dendrimer-based multifunctional conjugate for cancer therapy: synthesis, characterization, and functionality. *Biomacromolecules* **2006**, *7*, 572–579.
- Thomas, T. P.; Majoros, I. J.; Kotlyar, A.; Kukowska-Latallo, J. F.; Bielinska, A.; Myc, A.; Baker, J. R., Jr. Targeting and inhibition of cell growth by an engineered dendritic nanodevice. *J. Med. Chem.* **2005**, *48*, 3729–3735.
- Majoros, I. J.; Thomas, T. P.; Mehta, C. B.; Baker, J. R., Jr. Poly(amidoamine) dendrimer-based multifunctional engineered nanodevice for cancer therapy. *J. Med. Chem.* **2005**, *48*, 5892–5899.
- Patri, A. K.; Myc, A.; Beals, J.; Thomas, T. P.; Bander, N. H.; Baker, J. R., Jr. Synthesis and in vitro testing of J591 antibody-dendrimer conjugates for targeted prostate cancer therapy. *Bioconjugate Chem.* **2004**, *15*, 1174–1181.
- Shukla, R.; Thomas, T. P.; Peters, J. L.; Desai, A. M.; Kukowska-Latallo, J.; Patri, A. K.; Kotlyar, A.; Baker, J. R., Jr. HER2 specific tumor targeting with dendrimer conjugated anti-HER2 mAb. *Bioconjugate Chem.* **2006**, *17*, 1109–1115.
- Shukla, R.; Thomas, T. P.; Peters, J.; Kotlyar, A.; Myc, A.; Baker, J. R., Jr. Tumor angiogenic vasculature targeting with PAMAM dendrimer-RGD conjugates. *Chem. Commun.* **2005**, 5739–5741.
- Yang, W.; Barth, R. F.; Wu, G.; Bandyopadhyaya, A. K.; Thirumagal, B. T.; Tjarks, W.; Binns, P. J.; Riley, K.; Patel, H.; Coderre, J. A.; Ciesielski, M. J. Fenstermaker boronated epidermal growth factor as a delivery agent for neutron capture therapy of EGF receptor positive gliomas. *Appl. Radiat. Isot.* **2004**, *61*, 981–985.
- Barth, R. F.; Wu, G.; Yang, W. L.; Binns, P. J.; Riley, K. J.; Patel, H.; Coderre, J. A.; Tjarks, W.; Bandyopadhyaya, A. K.; Thirumagal, B. T.; Ciesielski, M. J.; Fenstermaker, R. A. Neutron capture therapy of epidermal growth factor gliomas using boronated cetuximab (IMC-C225) as a delivery agent. *Appl. Radiat. Isot.* **2004**, *61*, 899–903.
- Low, P. S.; Hene, W. A.; Doorneweerd, D. D. Discovery and Development of Folic Acid-Based Receptor Targeting for Imaging and Therapy of Cancer and Inflammatory Diseases. *Acc. Chem. Res.* **2008**, *41*, 120–129.
- Salazar, M. D.; Ratnam, M. The folate receptor: What does it promise in tissue targeted therapeutics? *Cancer Metastasis Rev.* **2007**, *26*, 141–152.
- Prateek, S.; Umesh, G.; Abhay, A.; Narendra, K. J. Folate and Folate-PEG-PAMAM Dendrimers: Synthesis, Characterization, and Targeted Anticancer Drug Delivery Potential in Tumor Bearing Mice. *Bioconjugate Chem.* **2008**, *19*, 2239–2252.
- Garin-Chesa, P.; Campbell, I.; Saigo, P.; Lewis, J.; Old, L.; Rettig, W. Trophoblast and ovarian cancer antigen LK26, sensitivity and specificity in immunopathology and molecular identification as a folate-binding protein. *Am. J. Pathol.* **1993**, *142*, 557–567.
- Lu, Y.; Low, P. S. Folate-mediated delivery of macromolecular anticancer therapeutic agents. *Adv. Drug Delivery Rev.* **2002**, *54*, 675–93.
- Wolinsky, J. B.; Grinstaff, M. W. Therapeutic and diagnostic applications of dendrimers for cancer treatment. *Adv. Drug Delivery Rev.* **2008**, *60*, 1037–1055.
- Beezer, A. E.; King, A. S. H.; Martin, I. K. Dendrimers as potential drug carriers; encapsulation of acidic hydrophobes within water soluble PAMAM derivatives. *Tetrahedron* **2003**, *59*, 3873–3880.
- Cheng, Y. Y.; Xu, T. The Effect of Dendrimers on the Pharmacodynamic and Pharmacokinetic Behaviors of Noncovalently or Covalently Attached Drugs. *Eur. J. Med. Chem.* **2008**, *43*, 2291–2297.
- Patri, A. K.; Kukowska-Latallo, J. F.; Baker, J. R., Jr. Targeted drug delivery with dendrimers: comparison of the release kinetics of covalently conjugated drug and noncovalent drug inclusion complex. *Adv. Drug Delivery Rev.* **2005**, *57*, 2203–2214.
- Myc, A.; Majoros, I. J.; Thomas, T. P.; Baker, J. R., Jr. Dendrimer-Based Targeted Delivery of an Apoptotic Sensor in Cancer Cells. *Biomacromolecules* **2007**, *8*, 13–18.
- Yang, W.; Cheng, Y. Y.; Xu, T.; Wang, X.; Wen, L. P. Targeting Cancer Cells with Biotin-Dendrimer Conjugates. *Eur. J. Med. Chem.* **2009**, *44*, 862–868.
- Hill, E.; Shukla, R.; Park, S. S.; Baker, J. R., Jr. Synthetic PAMAM-RGD Conjugates Target and Bind To Odontoblast-like MDPC 23 cells and the Predentin in Tooth Organ Cultures. *Bioconjugate Chem.* **2007**, *18*, 1756–1762.
- Lesniak, W. G.; Muhammed, S. T.; Nair, B. M. Synthesis and Characterization of PAMAM Dendrimer-Based Multifunctional Nanodevices for Targeting  $\alpha_v\beta_3$  Integrins. *Bioconjugate Chem.* **2007**, *18*, 1148–1154.
- Shi, X.; Wang, S.; Meshinchi, S.; Van, A. M. E.; Bi, X.; Lee, I.; Baker, J. R., Jr. Dendrimer-Entrapped Gold Nanoparticles as a Nanoplatforform for Cancer-Cell Targeting and Imaging. *Small* **2007**, *3*, 1245–1252.
- Shi, X.; Majoros, I. J.; Patri, A. K.; Bi, X.; Islam, M. T.; Ankur, D.; Rose Ganser, T.; Baker, J. R., Jr. Molecular heterogeneity analysis of poly(amidoamine) dendrimer-based mono- and multifunctional nanodevices by capillary electrophoresis. *Analyst* **2006**, *131*, 374–381.
- Kobayashi, H.; Sato, N.; Saga, T.; Nakamoto, Y.; Ishimori, T.; Toyama, S.; Togashi, K.; Konishi, J.; Brechbiel, M. W. Radiolabeling of Avidin with Very High Specific Activity for Internal Radiation Therapy of Intraperitoneally Disseminated Tumors. *Eur. J. Nucl. Med.* **2000**, *27*, 1334–1336.
- Kobayashi, H.; Wu, C.; Kim, M. K.; Paik, C. H.; Carrasquillo, J. A.; Brechbiel, M. W. Evaluation of the in Vivo Biodistribution of Indium-111 and Yttrium-88 Labeled Dendrimer-1B4M-DTPA and Its Conjugation with Anti-Tac Monoclonal Antibody. *Bioconjugate Chem.* **1999**, *10*, 103–111.
- Wu, C.; Brechbiel, M. W.; Kozak, R. W.; Gansow, O. A. Metal-chelate-dendrimer-antibody constructs for use in radioimmunotherapy and imaging. *Bioorg. Med. Chem. Lett.* **1994**, *4*, 449–454.
- Roberts, J. C.; Adams, Y. E.; Tomalia, D.; Mercer-Smith, J. A.; Lavallee, D. K. Using starburst dendrimers as linker molecules to radiolabel antibodies. *Bioconjugate Chem.* **1990**, *1*, 305–308.
- Sato, N.; Park, C. W.; Kim, H. S.; Han, E. K.; Wong, K. J.; Paik, R. S.; Park, L. S.; Yao, Z.; Carrasquillo, J. A.; Paik, C. H. Synthesis of dendrimer-based biotin radiopharmaceuticals to enhance whole-body clearance. *Nucl. Med. Biol.* **2003**, *30*, 617–625.
- Mamede, M.; Saga, T.; Kobayashi, H.; Ishimori, T.; Higashi, T.; Sato, N.; Brechbiel, M. W.; Konishi, J. Radiolabeling of Avidin with Very High Specific Activity for Internal Radiation Therapy of Intraperitoneally Disseminated Tumors. *Clin. Cancer Res.* **2003**, *9*, 3756–3762.
- Cristina, M.; August, S. P.; Roger, S. Synthesis and in Vitro/in Vivo Evaluation of Novel  $^{99m}\text{Tc}(\text{CO})_3$ -Folates. *Bioconjugate Chem.* **2006**, *17*, 797–806.
- Zhang, Y. Q.; Sun, Y. H.; Xu, X. P.; Zhu, H.; Huang, L. L.; Zhang, X. Z.; Qi, Y. J.; Shen, Y. M. Radiosynthesis and micro-SPECT

- imaging of  $^{99m}\text{Tc}$ -dendrimer poly(amido)-amine folic acid conjugate. *Bioorg. Med. Chem. Lett.* **2010**, *20*, 927–931.
- (39) Liu, M.; Xu, W.; Xu, L. J.; Zhong, G. R.; Chen, S. L.; Lu, W. Y. Synthesis and Biological Evaluation of Diethylenetriamine Pentaacetic Acid–Polyethylene Glycol–Folate: A New Folate-Derived,  $^{99m}\text{Tc}$ -Based Radiopharmaceutical. *Bioconjugate Chem.* **2005**, *16*, 1126–1132.
- (40) Katsuhiko, S.; Kentaro, H.; Mikako, O.; Junichiro, A.; Kengo, I. Radiosynthesis and in vivo evaluation of  $N$ -[ $^{11}\text{C}$ ]methylated imidazopyridineacetamides as PET tracers for peripheral benzodiazepine receptors. *Nucl. Med. Biol.* **2008**, *35*, 327–334.
- (41) Majoros, I. J.; Myc, A.; Thomas, T.; Mehta, C. B.; Baker, J. R., Jr. PAMAM Dendrimer-Based Multifunctional Conjugate for Cancer Therapy: Synthesis, Characterization, and Functionality. *Bio-macromolecules* **2006**, *7*, 572–579.
- (42) Durairaj, C.; Ramakrishna, S.; Farhan, J. A.; Roop, K. K.; Prakash, V. D. Folate coupled poly(ethyleneglycol) conjugates of anionic poly(amidoamine) dendrimer for inflammatory tissue specific drug delivery. *J. Biomed. Mater. Res., Part A* **2007**, 92–103.
- (43) Selhub, J.; Franklin, W. A. The folate binding protein of rat kidney. *J. Biol. Chem.* **1984**, *259*, 6601–6606.
- (44) Selhub, J.; Emmanouel, D.; Stavropoulos, T.; Arnold, R. Renal folate adsorption and the kidney folate binding protein. I. Urinary clearance studies. *Am. J. Physiol.* **1987**, *252*, F750–F756.
- (45) Selhub, J.; Nakamura, S.; Carone, F. A. Renal folate adsorption and the kidney binding protein. II. *Am. J. Physiol.* **1982**, *252*, F757–F760.
- (46) Williams, W. M.; Huang, K. C. Renal tubular transport of folic acid and methotrexate in the monkey. *Am. J. Physiol.* **1982**, *272*, F757–F760.
- (47) Jolanta, F. K.L.; Kimberly, A. C.; Cao, Z. Y.; Baker, J. R., Jr. Nanoparticle Targeting of Anticancer Drug Improves Therapeutic Response in Animal Model of Human Epithelial Cancer. *Cancer Res.* **2005**, *65* (12), 5317–5324.
- (48) Olga, A.; Aviva, T. H.; Alberto, G.; Dan, G. Folate-Targeted PEG as a Potential Carrier for Carboplatin Analogs. Synthesis and in Vitro Studies. *Bioconjugate Chem.* **2003**, *14*, 563–574.
- (49) Sudimach, B. A. J.; Lee, R. J. Targeted drug delivery via the folate receptor. *Adv. Drug Delivery Rev.* **2000**, *41*, 147–162.
- (50) Wang, X.; Shen, F.; Freisheim, L. H.; Gentry, L. E.; Ratnam, M. Differential stereospecificities and affinities of folate receptor isoforms for folate compounds and antifolates. *Biochem. Pharmacol.* **1992**, *44*, 1898–1901.
- (51) Maziarz, K. M.; Monaco, H. L.; Shen, F.; Ratnam, M. Complete mapping of divergent amino acids responsible for differential ligand binding of folate receptors alpha and beta. *J. Biol. Chem.* **1999**, *274*, 11086–11091.